UNIVERSIDAD NACIONAL DE COLOMBIA
SEDE MEDELLÍN
FACULTAD DE MINAS

DYNA
http://dyna.medellin.unal.edu.co/

Developing a fast cordless soldering iron via induction heating

Ernesto Edgar Mazón-Valadez [a], Alfonso Hernández-Sámano [a], Juan Carlos Estrada-Gutiérrez [a], José Ávila-Paz [a] & Mario Eduardo Cano-González [a*]

[a] *Centro Universitario de la Ciénega, Universidad de Guadalajara, Guadalajara, México. mazon_valadez@hotmail.com, h.s.alfonso@gmail.com, jcarlosredes@gmail.com, jocmos@hotmail.com, meduardo2001@hotmail.com*.*

Received: January 19th, de 2014. Received in revised form: June 10th, 2014. Accepted: October 17th, 2014

Abstract
This study aims to present the design of a new soldering iron for welding electronic components that work via AC magnetic fields. Moreover, the device has been designed to operate in cordless mode. The system comprises of a resonant inverter that is capable of generating an alternating magnetic field of 250 kHz in the center of a coil of 11 wires. The heating element is a cylindrical piece of ferromagnetic stainless steel with a concentric core of copper, which is maintained in contact with a standard and commercial tip. Additionally, we determined the power factor and the efficiency of the energy transfer with a maximum power consumption of 134 watts. The system represents a good tool suitable for the realization of development boards or electronic tasks.

Keywords: Electromagnetic induction, Heating, Resonant inverter, Soldering.

Desarrollo de un cautín inalámbrico rápido a través de calentamiento por inducción

Resumen
Se presenta el desarrollo de un dispositivo para soldar componentes electrónicos, el cual funciona a base de campos magnéticos alternos. El dispositivo ha sido diseñado para trabajar sin cableado. El nuevo soldador se compone de un inversor resonante capaz de generar campos magnéticos alternos de 250 kHz en el centro de una bobina de 11 espiras. El elemento calefactor es una pequeña pieza cilíndrica de acero inoxidable magnético con un núcleo concéntrico de cobre, el cual se encuentra unido a una punta reemplazable para cautín comercial. Adicionalmente hemos determinado el factor de potencia y la eficiencia en la transferencia de energía con un máximo de consumo de potencia de 134 Watts. El dispositivo representa una buena herramienta adecuada para la realización de tarjetas impresas para circuitos o tareas de electrónica.

Palabras clave: Inducción Electromagnética, Calentamiento, Inversor Resonante, Soldador.

1. Introduction

The induction heating process is a physical phenomenon that is widely used for the fast heating of ferromagnetic materials. A focalized distribution of eddy currents on the material is the origin of a quick heating [1]. Indeed, this kind of heating is cleaner than the conventional method of electric resistances as it does not involve any contact with the material [2]; nevertheless, the use of resistances implies a simpler technology and lower manufacturing cost.

At present, induction heaters are used in industrial applications for metallic pieces, such as dilatation, furnacing and welding [3]. Moreover, it is also used in daily life tasks, such as cooking [4], sealing plastic bags [5], and ironing clothes [6]. Other new applications are focused on the heating of magnetic iron oxide nanoparticles for the treatment of tumors [7] and for the study of the specific absorption rate of magnetic materials [8].

On the other hand, there are two types of soldering irons (guns or pencil presentations) especially designed to perform the welding of electronic components on printed circuit boards (PCB), mostly in electronic labs. The more common ones are mainly composed of an electrical resistance wrapped around a heating element that transmits the heat to a soldering tip to melt the wire of lead/tin. However, in the last few years, it has been possible to acquire high frequency soldering irons that work by using magnetic induction [9]. Due to a very different physical

principle, these devices exhibit a higher performance to melt the wire in contrast to the devices of resistance. These presentations of soldering irons (with resistances or induction) possess a cable directly connected to a domestic tension line or a control station. This fact represents a source of possible accidents, imprecise welds or an obstacle in the soldering process. In order to tackle this issue, the present work aims to develop a cordless soldering iron via induction heating. This device is a powerful tool, which allows comfortable welding, and is a good alternative for the development of tasks in the electronic lab.

2. Theoretical Background

2.1. Induction heating

The AC current flow in a cylindrical conductor rod with radius *a* have been studied for several years [10]. In case the conductor has ferromagnetic properties, this current flow could be induced by AC magnetic fields, producing a rapid heating in the material, formed by the distribution of eddy currents [1]. Fig. 1 shows the typical procedure to heat a ferromagnetic piece placed inside the region of a magnetic flux. The magnetic field is generated by the use of a coil with *N* loops and inductance *L*, which is powered with an AC power supply of high frequency. Moreover, the magnetic permeability of the metal depends on the temperature; indeed, the ferromagnetic ordering of the material could vanish in the Curie point (Curie temperature T_C) where it becomes a paramagnetic material [11,12].

In agreement with Brown [13], the magnitude of the magnetic field intensity *H* in the rod satisfies eq. (1).

$$\frac{d^2H}{dr^2}+\frac{1}{r}\frac{dH}{dr}-H(j2\pi f\mu\sigma)=0, \tag{1}$$

where, f is the frequency, μ is the magnetic permeability and σ is the conductivity of the material.

The solutions of eq. (1) are the typical Bessel functions of first class and order zero $H=AJ_0\left(r\sqrt{-j2\pi f\mu\sigma}\right)$, which describes an oscillatory behavior of H(r) in r = 0.

This solution can be rewritten as shown in eq. (2) [13].

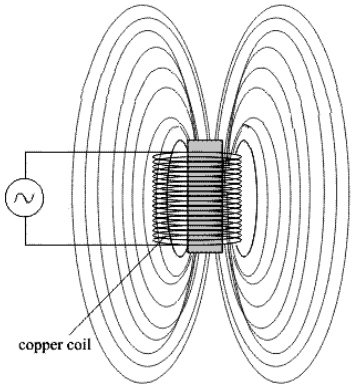

Figure 1. A ferromagnetic rod or cylinder heated with an AC magnetic field.
Source: Own

$$H=AJ_0(\sqrt{-2j}\,\frac{r}{s}), \tag{2}$$

where, $s=1/\sqrt{\pi f\mu\sigma}$ is physically known as the penetration of the radiofrequency (skin thickness) in the material [14], and the constant *A* depends on the initial conditions. With the new variables in eq. (2), it is possible to obtain the solution as a function of the radius of the cylinder and the skin thickness.

The relationship between the electric field due to the induced currents in the material and the magnetic field intensity is given in eq. (3). This expression can be obtained from the Maxwell-Ampere equation [15] neglecting the dielectric component of the material.

$$\frac{1}{\sigma}\frac{dH}{dr}=E. \tag{3}$$

Then, it is possible to determine the power dissipated ($p=\sigma E^2$) for the ferromagnetic rod in watts per unit length, as expressed in eq. (4) [15].

$$P=\int_{r=0}^{r=a}2\pi r\sigma E^2dr. \tag{4}$$

With a further analysis using the Frobenius solution of *H*, assuming uniform magnetic field intensity H_0 in all the metal and imposing boundary conditions on the surface of the cylinder, the value of *A* is determined. Thus, *P* is obtained in two ranges of (*a/s*) as shown in eqs. (5) and (6) [13].

$$P=\frac{2\pi H_0^2}{\sigma}\left(\frac{a}{s}\right)^4; \qquad \frac{a}{s}<1, \tag{5}$$

and

$$P=\frac{8\pi H_0^2}{\sigma}\frac{a}{s}; \qquad \frac{a}{s}>5. \tag{6}$$

Among the two equations, eq. (6) is more commonly used in industrial applications of induction heating; besides, the design of the heaters must take into account the values of μ and σ of the materials in order to establish the frequency range for heating. For example, if the goal is to heat a 1 cm diameter magnetic stainless steel rod, considering the definition of *s*, the regime $(a/s>5)$ and the values of $\mu = 1.76\times10^{-5}$ N A^{-2} and $\sigma = 1.45\times10^{6}$ Siemens/m, respectively, the minimum frequency suitable to heat is 100 Hz. If we increase the frequency, the material will also be heated and the skin will diminish. This material is a good electrical conductor but a bad conductor of heat, whereas copper has a high σ, a low μ, and transmits heat very quickly and high frequencies are needed [13].

2.2. Resonant inverter

Various configurations of switching circuits can be designed to generate AC magnetic fields. The resonant inverters are a good alternative to obtain AC current. They could be composed of an H-bridge (full or half) or "push pull" configurations of transistors to feed a series or parallel *LC* circuit or "tank" [16]. The tank resonates when the difference between the capacitive and the inductive reactance is null. The commutation ON/OFF of the transistors is carried out using a driver circuit. In some applications, a phase follower stage (PLL) or frequency compensation is also needed [17,18]. Indeed, various reports have shown that the resonant inverters can be used as correctors of power factor under certain operating conditions [19,20].

The half H-bridge inverter (Fig. 2) is an attractive choice in low-power and high-frequency applications as it exhibits good stability and simple topology to feed L-C, C-L-C or L-C-L resonant circuits with low total harmonic distortion. Fig. 2 shows a well-known resonant inverter (half or full bridge) [21,22], which feeds a C_R-L_R parallel circuit with correct impedance coupling through C_M-L_M circuit. The capacitor C_M limits the current to the resonant tank (C_R-L_R) and diminishes unwanted DC voltages. The inductor L_M is a filter for higher frequencies and gives the initial impulse to the tank circuit in each cycle of commutation. This resonant inverter also contains identical zener diodes to maintain the rectangular shape of the pulse, opposite identical ultrafast diodes to drain the back-electromotive forces and RC snubber circuits to suppress voltage transients returning from the tank. It is important to note that the maximum current value and magnetic field of the tank, in ideal conditions, satisfy eqs. (7) and (8), respectively; whereas, the frequency is approximate by eq. (9).

$$I_R = \frac{V_{DC}\sqrt{C_R}}{\sqrt{L_R}}. \tag{7}$$

$$B_{\text{Max}} = \frac{\mu_0 I_{\text{RMax}} N}{h}. \tag{8}$$

$$f_R = \frac{1}{2\pi\sqrt{L_R C_R}}. \tag{9}$$

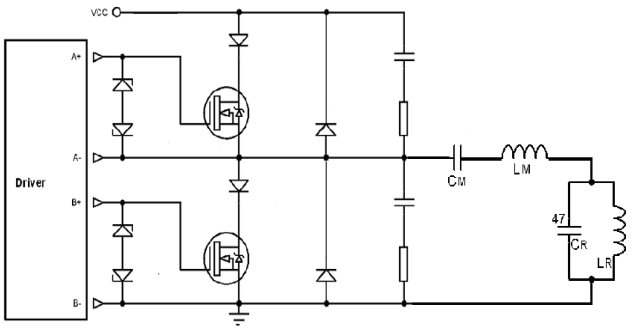

Figure 2. Diagram of a resonant inverter L-C-L with a half H-bridge.
Source: Own

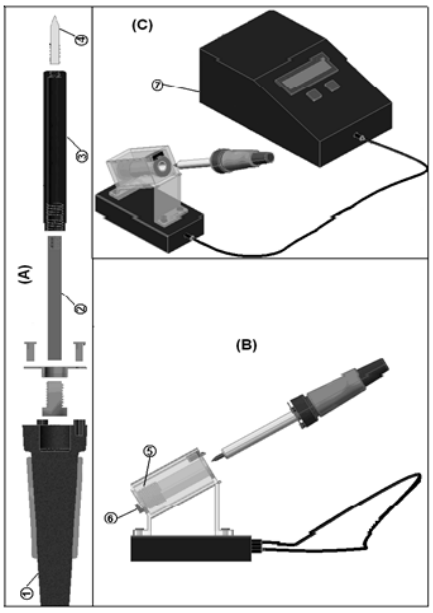

Figure 3. (A) New soldering iron with all the pieces, (B) lateral view of the soldering iron and the support with the resonant coil (5) and sensor (6), and (C) the full device including the control box (7).
Source: Own

3. Materials and Methods

3.1. The industrial design of the soldering iron

Initially, we used the handle of a commercial soldering iron with pencil design based on a resistance; thus, a new set of pieces was adapted to work via magnetic induction. Fig. 3(A) shows the design of the new soldering iron, which contains a thermal insulating handle (1), a thin cylindrical piece of copper (2), a thick cylindrical piece of magnetic stainless steel (3) and a standard tip (4).

The piece (3) is heated by the resonant inverter and works like a small thermal reservoir due to its diameter and low thermal conductivity. A radial heating is received by the concentric cylinder (2) and is quickly transferred to the tip (4). Fig. 3(B) shows a lateral view of the new soldering iron and its station. In this station, there is an AC magnetic field generator (5) to heat an extreme (3) and an infrared sensor (6). Fig. 3(C) exhibits the full system including the control box (7). In the coil (5), we have winding Litz wire on a rod of fiberglass to diminish the heating on the copper due to the skin thickness and support the temperature of the soldering iron, respectively [23].

3.2. Electronic features of the soldering iron

In order to develop the cordless soldering iron, we used a resonant inverter, like the one shown in Fig. 2 but without snubbers, transistors STW14NK50Z (MOSFET technology) of very low cost and the passive components C_M = 300 nF, L_M = 10 µH, C_R = 188 nF, and L_R = 2.15µH. The device also contains a microcontroller (MCU) PIC18F4550 for driving the inverter, to digitizing and displaying the temperature readings. Initially, the MCU produces two digital control signals with a 60% duty cycle, 250 kHz frequency with 180° of phase shift and a delay of 0.5 µs between them.

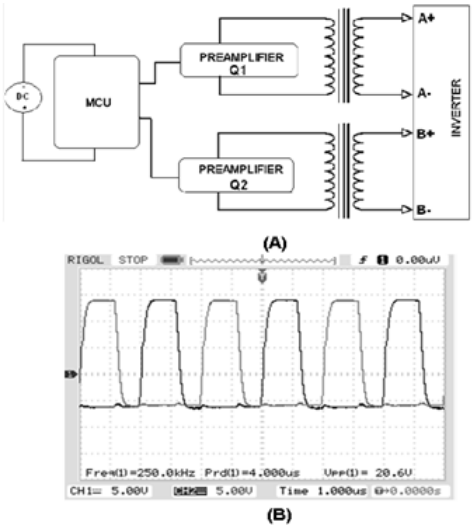

Figure 4. (A) Block diagram of the driver and (B) corresponding output signal of the driver.
Source: Own

The pulses are pre-amplified with a pair of MOSFETs BS170 to feed an isolation transformer of 45 turns. Next, each signal is an input of the MOSFET driver UCC37321P and UCC37322P, respectively, to invert each one. Then, the stages of low and high powers are galvanically isolated. Fig. 4(A) shows the block diagram of the driver circuit, while Fig. 4(B) shows the signals to switch the current in the inverter obtained from the oscilloscope and measured in each gate of the transistor. These signals have rectangular shape with a 40% duty cycle and 0.5 μs dead time. The negative amplitude of the signal guarantees the fast cut-off of the transistors, whereas the positive one ensures its saturation status.

In order to have a continuous monitoring of the welding tip temperature, an infrared thermopile MLX90616 is calibrated. This sensor is connected to an integrator and a non-inverting amplification using operational amplifiers. The total gain of the amplification is 7.3 and the circuit is shown in Fig. 5. Protection of the device is essential for having control on the maximum temperature of the stainless steel, since a strong diminution of the resonant charge could damage the circuits. This fact becomes very critical when the temperature in (3) reaches the value $T = T_C$, or when the user heats different materials with the same resonant coil. Our observations in the range from room temperature to 500°C of the inductance allow a maximum increasing of 5%. For this reason, an electronic stage of frequency compensation or PLL circuits can be neglected, but it is also needed to turn-off the system when the soldering iron has been removed.

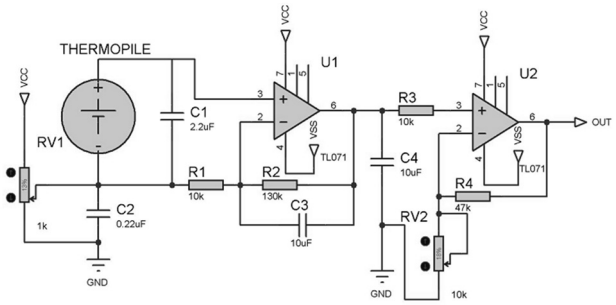

Figure 5. Amplification circuit of the thermopile infrared sensor.
Source: Own

The DC power supply of the inverter has been constructed using EMI/RFI filter to avoid any interference with other equipments [24], then the AC current is rectified by four diodes, and another LC filter (150 μH and 1 μF) is added to increase the power factor; besides, we observed a diminution of the total harmonic distortion in the output current. Fig. 6 shows the schematic circuit.

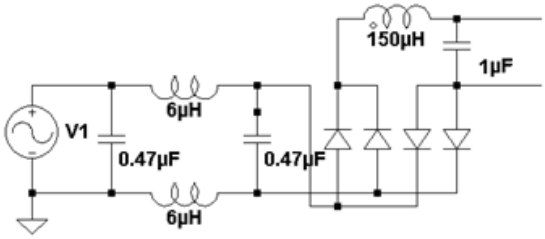

Figure 6. Schematic diagram of the DC power supply.
Source: Own.

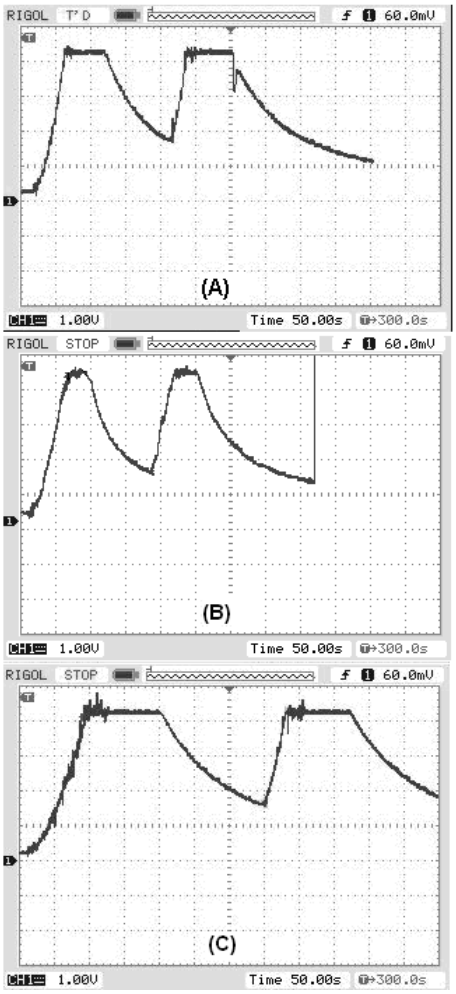

Figure 7. Welding cycles with (A) d_e = 0.762 cm, (B) d_e = 0.889 cm, and (C) d_e = 1.016 cm.
Source: Own

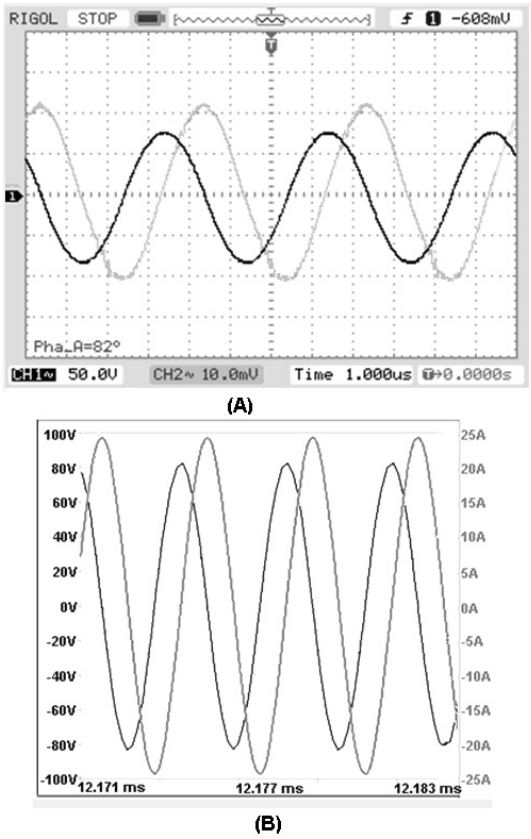

Figure 8. (A) Curves of voltage (black line) and current (gray line) obtained experimentally and (B) ideal curves simulated with the LT-Spice.
Source: Own

4. Experimental Results and Discussions

With the aim of establishing a "welding cycle", we studied the heating of the tip with various diameters of the stainless steel piece (3) as shown in Fig. 3(A). The readings of the infrared sensor were obtained using the oscilloscope with scales of 50 s/div and 120°C/div.

Fig. 7 exhibits the welding cycles considering external diameters d_e of 0.762 cm, 0.889 cm and 1.016 cm. For example, with d_e = 0.762 cm and starting from room temperature (25°C), the value T = 500°C is reached in 45 s. This value is maintained for a time lapse, before the inverter is turned off and the temperature diminishes to reach T = 200°C in 90 s. At this point, it is not possible to melt the welding wire, but by turning on the inverter, the tip again reaches T = 500°C in 20 s. Thus, ideally, we have 20 s to heat the tip and 90 s for soldering electronic components. We chose d_e = 1.016 cm, with a cycle 32 s to heat, 155 s for soldering and initial heating of 80 s, the latter is similar to the initial heating time of a commercial soldering iron with resistance (pencil).

Following with the characterization of the device, using a current probe of Hall Effect A6303 with its corresponding amplifier AM 503 connected to an oscilloscope, the curves of voltage and current in the resonant tank were studied while the tip was heated. Fig. 8(A) shows a sinusoidal shape of 250 kHz in the current (0.5 A/mV) and voltage (50 V/div), with maximum RMS value of 16.26 A and 56.57 V, respectively. Moreover, a phase shift of 82° was observed. These measurements exhibit a good agreement with the ideal values simulated in the LT-Spice platform shown in Fig. 8(B). Furthermore, a very small distortion was observed in the current signal.

Fig. 9(A) shows the signal of the current (1 A/mV) in a larger interval, which is modulated in amplitude, the modulating signal is 60 Hz of the domestic line tension. This observation is also in a good agreement with the theoretical predictions of the simulation shown in Fig. 9(B). The main difference is in the zero crossing, but this is due to the capacitance of the LC circuit to correct the power factor.

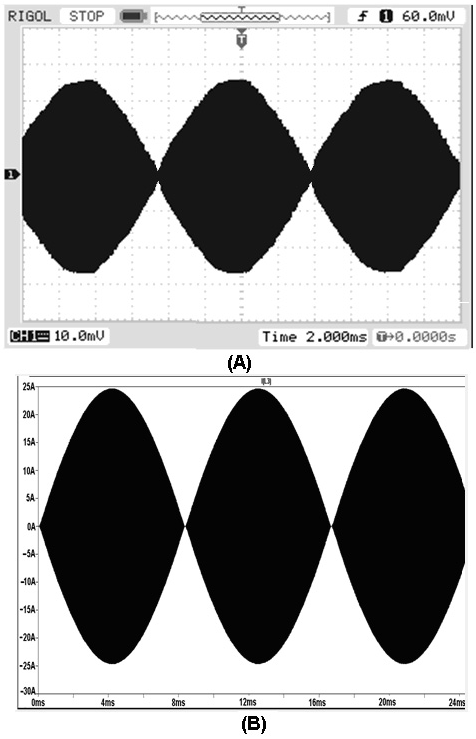

Figure 9. (A) Curves of current obtained experimentally and (B) simulated with the LT-Spice.
Source: Own

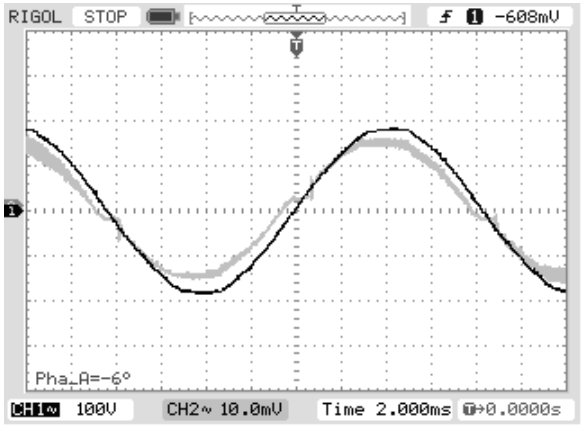

Figure 10. Curves of the current (gray line) consumption and voltage (dark line) obtained experimentally.
Source: own

Additionally, in order to study the power consumption of the device, the curves of current and voltage in the input were also analyzed. Fig. 10 shows those curves in the scale of (0.1 A/mV) and (100 V/div). In those measurements, a phase shift $\theta = -6º$ is observed, which allows a power factor $Cos\theta = -6º = 0.995$, current consumption I_{RMS} = 1.06 A with v_{RMS} = 127 V.

We analyzed the efficiency with a simple calculus of the maximum input and output power of the device; this value is given by eq. (10).

$$\eta = \frac{P_{output}}{P_{input}}, \tag{10}$$

where, P_{input} and P_{output} satisfy eqs. (11) and (12), respectively.

$$P_{input} = I_{input} V_{input} \cos\theta_{input}. \tag{11}$$

$$P_{output} = I_{out} V_{out} \cos\theta_{out}. \tag{12}$$

Regarding the RMS values shown in Figs. 8(A) and 10, P_{output} = 128 W, P_{input} = 134 W and η =95.5%.

5. Conclusions

In this study, we designed and built a new and efficient soldering iron with pencil presentation and replaceable tips, which works via high frequency induction heating. Moreover, the pencil does not contain any cord to the power supply in order to avoid accidents in the welding process. The device was developed using a resonant inverter with half H-bridge topology controlled using a microcontroller.

The microcontroller reads the temperature of the tip and turns off the device before it reaches the Curie temperature or if the pencil is removed. The device is characterized by determining its curvers of input and output current and voltage. It exhibits an acceptable power factor and efficiency of 95.5% and a low total harmonic distortion. Furthermore, the device is built using low cost components. It represents a suitable alternative in the welding tasks in comparison to the current devices based on resistances. Indeed, the device is currently being used in our Biophysics lab and has proved to be a very useful tool for welding fragile electronic components on PCBs. Our observations indicate that with the "welding cycle" chosen, an experienced electronics technician may perform up to 45 welds per cycle.

Acknowledgments

All the authors are grateful to the Mexican institution CONACYT for its valuable support.

References

[1] Field, A. B. Eddy Currents in large Slot-Wound conductors. American Institute of Electrical Engineers, Transactions of the 26, pp. 761-788, 1905.

[2] Boadi, A., Tsuchida,Y., Todaka,T. and Enokizono, M. Designing of suitable construction of high-frequency induction heating coil by using finite-element method. Magnetics. IEEE Transactions, 41(10), pp. 4048–4050, 2005.

[3] Bayındır, N.S., Kükrer, O. and Yakup, M. DSP-based PLL-controlled 50–100 kHz 20 kW high frequency induction heating system for surface hardening and welding applications. IEE Proceedings - Electric Power Applications, 150(3), pp. 365-371, 2003. http://dx.doi.org/10.1049/ip-epa:20030096

[4] Burdío, M., Monterde, F., Garcia, J. R., Barragan, L. A. and Martinez, A. A two-output series-resonant inverter for inductionheating cooking appliances. Power Electronics, IEEE Transactions on, 20(4), pp. 815-822, 2005.

[5] Grooms, J. P., Mattson, L. J., Method for induction sealing an inner bag to an outer container, US 5416303A, 16 May 1995.

[6] Lung W. Ch. Induction ironing apparatus and method, US 7681342 B2, 9 October 2006

[7] Jordan, A., Scholz, R., Maier-Hauff, K., Johannsen, Wust, M., Nadobny, P. J., Schirra, H., Schmidt, H., Deger, S., Loening, S., Lanksch, W. and Felix, R. Presentation of a new magnetic field therapy system for the treatment of human solid tumors with magnetic fluid hyperthermia. Journal of Magnetism and. Magnetic. Materials, 225 (1–2), pp. 118–126, 2001. http://dx.doi.org/10.1016/S0304-8853(00)01239-7

[8] Cano, M. E., Barrera, A., Estrada, J. C., Hernandez, A. and Córdova, T. An induction heater device for studies of magnetic hyperthermia and specific absorption ratio measurements. Review of Scientific Instruments, 82 (11), pp. 114904-114904-6, 2011. http://dx.doi.org/10.1063/1.3658818

[9] Mitsuhiko M.. System and Method for Induction Heating of a Soldering Iron, US/2010/0258554 A1, October 14 of 2010.

[10] Snown, C., Alternating current distribution in cylindrical conductors, in: Scientific Papers of the Bureau of Standards, 20, Washington, USA, pp. 277-338, 1925.

[11] Buschow, K. H. J. Encyclopedia of Materials: Science and Technology.Michigan: University of Michigan, vol 8, Elsevier, 2001. http://dx.doi.org/10.1016/B0-08-043152-6/00016-4, http://dx.doi.org/10.1016/B0-08-043152-6/01367-X, http://dx.doi.org/10.1016/B0-08-043152-6/00841-X

[12] Kittel, C. Introduction to Solid State Physics, New York: John Wiley & Sons, 6th ed, 1986.

[13] Brown, G. H., Hoyler, C. N., Bierwirth, R. A., Theory and Applications of the Radiofrequency Heating, New York: D. Van Nostrand Company, 1947.

[14] Dwight, H. B, A Precise Method of Calculation of Skin Effect in Isolated Tubes. Journal of the American Institute of Electrical Engineers, 42(8), pp. 830, 1923. http://dx.doi.org/10.1109/JoAIEE.1923.6593471

[15] Jackson, J.D., Classical Electrodynamics, 3rd ed., Wiley, New York, 1998.

[16] Llorente, S., Monterde, F., Burdio, J.M., Acero, J., A comparative study of resonant inverter topologies used in induction cookers, Applied Power Electronics Conference and Exposition, 7th. Annual IEEE, pp.1168-1174, 2002.

[17] Calleja, H., Fast Response Control Circuit for Resonant Inverters, International Journal of Electronics, 89(3), pp. 233-244, 2002. http://dx.doi.org/10.1080/00207210210122550

[18] Kamli, M., Yamamoto, S. and Abe, M., A 50-150 kHz Half-Bridge Inverter for Induction Heating Applications.IEEE Transactions on Industrial Electronics, 43(1), pp. 163–172, 1996. http://dx.doi.org/10.1109/41.481422

[19] Kawamura,Y., TokiwaM., Kim Y.J., Nakaoka, M., New induction heated fluid energy conversion processing appliance incorporating auto-tuning PID control-based PWM resonant IGBT inverter with sensorless power factor correction, Power Electronics Specialists Conference, Record., 26th Annual IEEE, pp.1191-1197, 1995.

[20] Calleja, H. and Ordonez, R., Induction heating inverter with active power factor correction. International Journal of Electronics, 86(9), pp. 1113-1121, 1999. http://dx.doi.org/10.1080/002072199132888

[21] Ye, Z., Jain, P. K. and Sen, P. C., Full-Bridge Resonant Inverter With Modified Phase-Shift Modulation for High-Frequency AC

Power Distribution Systems, IEEE Transactions on Industrial Electronics, 54 (1), pp. 2831-2845, 2007.
[22] Goya Gerardo Fabian, Cassinelli Nicolas, Ibarra García Manuel Ricardo, Magnetic Hyperthermia Application Device, PCT/ES2009/000235, November 12 of 2009.
[23] Lacroix, L.M., Carrey, J. and Respaud, M., A frequency-adjustable electromagnet for hyperthermia measurements on magnetic nanoparticles, Review of Scientific Instruments, 79(9), pp. 093909-093909-5, 2008. http://dx.doi.org/10.1063/1.2972172
[24] Tai, C. C., Cheng, M. K., Anti-interference Design of Quasi-resonant Tank for Magnetic Induction Heating System. PIERS Online, 4(4), pp. 417-420, 2008. http://dx.doi.org/10.2529/PIERS070907021437

E.E. Mazón-Valadez, received, the BIE degree in 2012 from the Universidad of Guadalajara, México, he is Student in the Masters in physics in the Centro Universitario de la Ciénega of the Universidad de Guadalajara, in México. His research interest include: Magnetic Hyperthermia, Resonant Inverters and SAR.

A. Hernández-Sámano, received the MPhys degree in 2013 from the University of Guanajuato, México, he is Student in the PhD in physics in the Centro Universitario de la Ciénega of the Universidad de Guadalajara, in México. His research interest include: Magnetic Hyperthermia, Resonant Inverters and Magnetometry.

J.C. Estrada-Gutiérrez, received the MComp. in 2005 from the Universidad of Guadalajara, México, Full Professor en the Technologic Sciences department in the Centro Universitario de la Ciénega of the Universidad de Guadalajara, in México. His research interest include: Magnetic Hyperthermia, Automation and Control and Embedded Systems.

J. Ávila-Paz, received MSc.in 2003 from the Universidad Central Marta Abreu de las Villas, Cuba, Full Professor in the Technologic Sciences department in the Centro Universitario de la Ciénega of the Universidad de Guadalajara, in México. His research interest include: Magnetic Hyperthermia, Automation and Control, and Embedded Systems.

M.E. Cano-González, received the PhD degree in Physics in 2007 from the University of Guanajuato, México. Full professor in the Basic Sciences department in the Centro Universitario de la Ciénega of the Universidad de Guadalajara, in México. His research interest include: Magnetic Hyperthermia, Resonant Inverters and Monte Carlo Simulations.